HHS Public Access

Author manuscript

Bone. Author manuscript; available in PMC 2024 December 01.

Published in final edited form as:

Bone. 2023 December ; 177: 116898. doi:10.1016/j.bone.2023.116898.

Antisense Oligonucleotides Targeting a NOTCH3 Mutation in Male Mice Ameliorate the Cortical Osteopenia of Lateral Meningocele Syndrome

Ernesto Canalis[1,2,3,*], **Magda Mocarska**[3], **Lauren Schilling**[3], **Paymaan Jafar-nejad**[4], **Michele Carrer**[4]

[1]Department of Orthopaedic Surgery, UConn Health, Farmington, CT, USA

[2]Department of Medicine, UConn Health, Farmington, CT, USA

[3]UConn Musculoskeletal Institute, UConn Health, Farmington, CT, USA

[4]Ionis Pharmaceuticals, Inc., Carlsbad, California, USA

Abstract

Lateral Meningocele Syndrome (LMS) is a monogenic disorder associated with *NOTCH3* pathogenic variants that result in the stabilization of NOTCH3 and a gain-of-function. A mouse model (*Notch3*^{em1Ecan}) harboring a 6691TAATGA mutation in the *Notch3* locus that results in a functional outcome analogous to LMS exhibits cancellous and cortical bone osteopenia. We tested Notch3 antisense oligonucleotides (ASOs) specific to the *Notch3*$^{6691\text{-}TAATGA}$ mutation for their effects on *Notch3* downregulation and on the osteopenia of *Notch3*^{em1Ecan} mice. Twenty-four mouse Notch3 mutant ASOs were designed and tested for toxic effects *in vivo*, and 12 safe ASOs were tested for their impact on the downregulation of *Notch3*$^{6691\text{-}TTATGA}$ and *Notch3* mRNA in osteoblast cultures from *Notch3*^{em1Ecan} mice. Three ASOs downregulated *Notch3* mutant transcripts specifically and were tested *in vivo* for their effects on the bone microarchitecture of *Notch3*^{em1Ecan} mice. All three ASOs were well tolerated. One of these ASOs had more consistent effects *in vivo* and was studied in detail. The Notch3 mutant ASO downregulated *Notch3* mutant transcripts in osteoblasts and bone marrow stromal cells and had no effect on other Notch receptors. The subcutaneous administration of Notch3 mutant ASO at 50 mg/Kg decreased *Notch*$^{6691\text{-}TTATGA}$ mRNA in bone without apparent toxicity; microcomputed tomography demonstrated that the ASO ameliorated the cortical osteopenia of *Notch3*^{em1Ecan}

[*]Address correspondence to: Ernesto Canalis, M.D., Department of Orthopedic Surgery, UConn Health, Farmington, CT 06030-4037, Telephone: (860) 679-7978; Fax: (860) 679-1474; canalis@uchc.edu.

CRediT authorship contribution statement

Ernesto Canalis: Conceptualization, Methodology, Validation, Writing – Original Draft, Writing – Review & Editing, Supervision, Project Administration, Funding Acquisition. **Lauren Schilling**: Investigation, Visualization. **Magda Mocarska**: Investigation. **Paymaan Jafar-nejad**: Resources, Writing – Review and Editing, Visualiztion. **Michele Carrer**: Resource, Writing – Review and Editing, Visualization.

Conflict of Interest

The authors declare no conflicts of interest with the contents of this article.

mice but not the cancellous bone osteopenia. In conclusion, a Notch3 ASO that downregulates *Notch3* mutant expression specifically ameliorates the cortical osteopenia in *Notch3*^{em1Ecan} mice. ASOs may become useful strategies in the management of monogenic disorders affecting the skeleton.

Keywords

Notch receptors; NOTCH3; gene mutations; antisense oligonucleotides; cortical bone; osteopenia

1. INTRODUCTION

Notch receptors (Notch1 through 4) are determinants of cell fate and function in multiple cellular organizations including the skeleton [1, 2]. *Notch1*, *2* and *3* and low levels of *Notch4* transcripts are detected in bone cells, where each receptor plays a distinct role influencing the fate of cells of the osteoblast and osteoclast lineages [3]. Interactions of Notch receptors with ligands of the Jagged and Delta-like families result in the cleavage of NOTCH and activation of signaling following the release of the NOTCH intracellular domain (NICD), and its translocation into the nucleus to induce the transcription of target genes [4–6]. These include genes encoding Hairy Enhancer of Split (HES)1, 5 and 7 and HES-related with YRPW motif (HEY)1, 2 and L [7].

Each Notch receptor has distinct patterns of cellular expression and activity and pathogenic variants associated with each receptor result in distinct clinical syndromes. *NOTCH3* is expressed in mural vascular cells where it plays a critical function in vascular homeostasis [8]. Pathogenic variants of *NOTCH3* associated with mutations in its extracellular domain cause cerebral autosomal dominant arteriopathy with subcortical infarcts and leukoencephalopathy (CADASIL) [8–11]. In bone, *Notch3* is expressed in osteocytes and osteoblasts and its activation in these cells increases intracortical bone remodeling [12].

Lateral meningocele syndrome (LMS), also known as Lehman Syndrome, (Online Mendelian Inheritance in Man 130720) is a devastating disorder associated with pathogenic variants of *NOTCH3* and presenting with meningoceles, distinct facial features, developmental delay, decreased muscle mass, cardiac valve defects, short stature, scoliosis and craniofacial abnormalities [13–16]. LMS is associated with mutations or deletions in exon 33 of *NOTCH3*, that result in the creation of a STOP codon upstream of sequences coding for the proline (P), glutamic acid (E), serine (S) and threonine (T) (PEST) domain. As a result, the PEST domain is not translated and NOTCH3 is presumably stable, and a gain-of-function occurs [14]. Autosomal dominant inheritance and de novo heterozygous mutations are reported. Treatment of LMS is not available. To understand mechanisms operating in the pathogenesis of LMS and develop potential therapeutic agents to influence the outcome of LMS, we created a mouse model, *Notch3*^{em1Ecan} (syn *Notch3*$^{tm1.1Ecan}$), that recapitulates the genetic variant from LMS. *Notch3*^{em1Ecan} mice harbor a 6691-TAATGA mutation in exon 33 that results in a STOP codon upstream of the PEST domain [17]. The mice exhibit a NOTCH3 gain-of-function, cortical and cancellous bone osteopenia [17].

A number of approaches have been devised to downregulate Notch signaling and could serve to temper conditions where a gain-of-function exits. Often Notch inhibitors are not specific for Notch signaling or specific to a given Notch receptor [18–23]. Antibodies to the negative regulatory region (NRR) of Notch have been effective at preventing the activation of individual Notch receptors, including NOTCH3, but they do not target the Notch pathogenic variants and as a consequence they downregulate wild type as well as the mutant Notch receptor [24–26].

The use of antisense oligonucleotides (ASO) is a novel therapeutic approach of RNA modulation, and ASOs have been effective in a variety of tissues including the central and peripheral nervous system, retina, liver, muscle and bone [27–36]. ASOs are single-stranded synthetic nucleic acids that bind target mRNA by Watson-Crick pairing resulting in mRNA degradation by RNase H [37, 38]. In previous studies, we employed the systemic administration of ASOs targeting either wild type *Notch2* or *Notch3* to downregulate these genes in mice harboring *Notch2* or *Notch3* mutations resulting in a gain-of-function [36, 39]. Although the approach was successful in ameliorating the osteopenia of both mouse models, the ASOs employed were not allele selective and they did not target the mutant gene specifically.

The purpose of the present work was to evaluate if by targeting the mutant allele in heterozygous *Notch3*^{em1Ecan} mice, we could preserve the wild type allele creating a more normal genetic outcome. Because *Notch3*^{em1Ecan} mice present with osteopenia, we asked whether a more favorable genetic outcome would ameliorate this aspect of the *Notch3*^{em1Ecan} phenotype. Ionis pharmaceuticals designed and synthesized ASOs that would target specifically the *Notch3*$^{6691\text{-}TAATGA}$ mutation harbored by the *Notch3*^{em1Ecan} mouse. Notch3 mutant specific ASOs were tested *in vitro* and *in vivo* for their tolerability and for effects on the downregulation of wild type and mutant *Notch3* transcripts and on the skeletal microarchitecture of heterozygous *Notch3*^{em1Ecan} mice.

2. MATERIALS AND METHODS

2.1 Notch3^{em1Ecan} Mutant Mice

Heterozygous *Notch3*^{em1Ecan} (syn *Notch3*$^{tm1.1Ecan}$) mice in a C57BL/6 genetic background were used to test the efficacy of ASOs *in vitro* and *in vivo*. *Notch3*^{em1Ecan} mice harbor a tandem termination at bases 6691–6696 (ACCAAG→TAATGA) in exon 33 of *Notch3* that results in the same functional outcome as the one found in LMS [17]. Genotypes were determined by PCR analysis of tail DNA using forward primer 5’-GTGCTCAGCTTTGGTCTGCTC-3’ and either reverse primer 5’-CGCAGGAAGCGCGCTCATTA-3’ for *Notch3*^{em1Ecan} mutant or 5’-CGCAGGAAGCGGGCCT TGG-3’ for the wild type allele (Integrated DNA Technologies, Coralville, IA). To characterize and study the effect of Notch3 ASOs in *Notch3*^{em1Ecan} mice, heterozygous *Notch3*^{em1Ecan} mutants were crossed with wild type mice to generate ~50% heterozygous *Notch3*^{em1Ecan} mice and 50% control littermates. Studies were approved by the Institutional Animal Care and Use Committee of UConn Health.

2.2 Notch3 Antisense Oligonucleotides

ASOs used in the current study consist of a central stretch of 10 DNA nucleotides flanked on either side by 3 nucleotides containing constrained ethyl (cEt) modifications. Additionally, the phosphodiester internucleotide linkages were replaced with phosphorothioate (PS). Twenty-four ASOs targeting the *Notch3*$^{6691\text{-}TAATGA}$ mutant pre-mRNA were designed in silico by Ionis Pharmaceuticals (Carlsbad, CA). ASOs covering at least one of the nucleotides that are mutated in the *Notch3*^{em1Ecan} mouse were designed (Figure 1). A control ASO that does not hybridize to any specific mRNA sequence was included in all experiments. Oligonucleotides were synthesized at Ionis Pharmaceuticals using an AKTA Oligopilot, as described previously [40]. Initially, 24 Notch3 mutant ASOs were tested for toxicity at Ionis Pharmaceuticals (Carlsbad, CA) in 8-week-old *BALB/c* mice. To this end, male mice were administered ASOs at a dose of 50 mg/Kg subcutaneously once a week for a total of 4.5 weeks (5 doses) and euthanized 72 h after the last dose of ASO. Body weights were determined weekly, and liver, kidney, and spleen were weighed after euthanasia and normalized to body weight and compared with organs from control mice. Blood was obtained by cardiac puncture, and plasma was collected for the measurement of alanine aminotransferase, aspartate aminotransferase, total bilirubin, albumin, and blood urea nitrogen. These procedures were performed at, and approved by, the Animal Care and Use Committee of Ionis Pharmaceuticals. Twelve well tolerated mouse ASOs targeting the mutant Notch3 sequence, and a control ASO that does not hybridize to any specific mRNA sequence, were selected for further study.

2.3 Osteoblast-enriched Cell Cultures

Osteoblasts were isolated following the digestion of parietal bones from 3 to 5 day old control and *Notch3*^{em1Ecan} mice with liberase TL 1.2 units/ml (Sigma-Aldrich St. Louis, MO) for 20 min at 37°C for 5 consecutive reactions [41]. The cells isolated from the last 3 digestions were pooled and seeded at a density of 10×10^4 cells/cm^2 [42]. Osteoblast-enriched cells were cultured in Dulbecco's modified Eagle's medium (DMEM) supplemented with non-essential amino acids (both from Thermo Fisher Scientific, Waltham, MA) and 10% heat-inactivated fetal bovine serum (FBS; Atlanta Biologicals, Norcross, GA) in a humidified 5% CO_2 atmosphere at 37°C. Confluent cells were exposed to DMEM supplemented with 10% heat-inactivated FBS, 100 μg/ml ascorbic acid and 5 mM β-glycerophosphate (both from Sigma-Aldrich) in the absence or presence of Notch3 mutant or control ASOs at various doses and periods of time as indicated in text and legends.

2.4 Bone Marrow Stromal Cell Cultures

Femurs and tibiae from 4 to 8 week old *Notch3*^{em1Ecan} mice and littermate controls were dissected, the epiphysis removed and bone marrow stromal cells recovered by centrifugation [43]. Cells were pooled and seeded at a density of 1.25×10^6 cells/cm^2 in α-minimum essential medium (α-MEM; Thermo Fisher Scientific) containing heat-inactivated 15% FBS and cultured at 37°C in a humidified 5% CO_2 incubator. At confluence, cells were exposed to α-MEM supplemented with 10% FBS, 100 μg/ml ascorbic acid and 5 mM β-glycerophosphate and cultured in the absence or presence of Notch3 mutant or control ASOs at distinct doses and periods of time as indicated in text and legends.

2.5 In vivo Administration of Notch3 ASOs

One month old male *Notch3*^{em1Ecan} heterozygous mutant and sex-matched wild type littermates were administered Notch3 mutant specific ASOs or control ASO suspended in PBS subcutaneously a dose of 50 mg/Kg once a week for 4 consecutive weeks to 1 month old *Notch3*^{em1Ecan} and control mice, and mice were euthanized at 2 months of age.

2.6 Microcomputed Tomography (μCT)

Bone microarchitecture of femurs from experimental and control mice was determined using a μCT 40 microcomputed tomography instrument (Scanco Medical AG, Bassersdorf, Switzerland), which was calibrated periodically using a phantom provided by the manufacturer [44, 45]. Femurs were placed in 70% ethanol and scanned at high resolution, energy level of 55 kVp, intensity of 145 μA and integration time of 200 ms. One hundred and sixty slices at the distal femoral metaphysis were acquired at an isotropic voxel size of 216 μm^3 and a slice thickness of 6 μm and chosen for analysis of cancellous bone microarchitecture. Trabecular bone volume fraction and microarchitecture were evaluated starting ~1.0 mm proximal from the femoral condyles. Contours were manually drawn a few voxels away from the endocortical boundary every 10 slices to define the region of analysis. The remaining slice contours were iterated automatically. Trabecular regions were assessed for total volume, bone volume, bone volume fraction (bone volume/total volume), trabecular thickness, trabecular number, trabecular separation, connectivity density and structure model index, using a Gaussian filter ($\sigma = 0.8$), and a threshold of 240 permil equivalent to 355.5 mg/cm^3 hydroxyapatite [44, 45]. Femoral cortical bone architecture was performed along the cortex of the femoral midshaft, excluding the marrow cavity. Contours were iterated across 100 slices and analysis of bone volume/total volume, porosity, cortical thickness, total cross-sectional and cortical bone area, and polar moment inertia were performed using a Gaussian filter ($\sigma = 0.8$, support = 1), and a threshold of 400 permil equivalent to 704.7 mg/cm^3 hydroxyapatite.

2.7 Quantitative Reverse Transcription-Polymerase Chain Reaction (qRT-PCR)

Total RNA was extracted from cells, homogenized femurs or tibiae, following the removal of the bone marrow by centrifugation with the RNeasy kit or microRNeasy Kit (Qiagen, Valencia, CA), in accordance with manufacturer's instructions [46–49]. The integrity of the RNA was assessed in random samples by microfluidic electrophoresis on an Experion instrument (BioRad, Hercules, CA), and only RNA with a quality indicator number equal to or higher than 7.0 was used for subsequent analysis. Equal amounts of RNA were reverse-transcribed using the iScript RT-PCR kit (BioRad) and amplified in the presence of specific primers (IDT) (Table 1A) with the iQ SYBR Green Supermix or SsoAdvanced Universal SYBR Green Supermix (BioRad) at 60°C for 35 cycles. Transcript copy number was estimated by comparison with a serial dilution of cDNA for *Notch1* (from J.S. Nye, Cambridge, MA), *Notch2* (from Thermo Fisher Scientific) and *Notch4* (from Y. Shirayoshi, Tottori, Japan) [50, 51]. *Notch3* wild type copy number was estimated by comparison to a serial dilution of a 100 to 200 base pair synthetic DNA template (IDT) cloned into pcDNA3.1 (Thermo Fischer Scientific) by isothermal single reaction assembly using commercially available reagents (New England BioLabs, Ipswich, MA) [52].

In experiments where cells or tissues were obtained from *Notch3*^{em1Ecan} mice with the intent to determine an ASO effect on *Notch3*$^{6691\text{-}TAATGA}$ mutant transcripts, fluorescent tagged products were used to perform RT-PCR. Total RNA was reverse transcribed with Moloney murine leukemia virus reverse transcriptase in the presence of reverse primers of *Notch3* (5'-ATAAGGATGCTCGC TGGGAACC-3') and *Rpl38* (Table 1A). *Notch3* cDNA was amplified by qPCR in the presence of SsoAdvanced Universal Probes Supermix (BioRad) gene expression assay mix, Notch3 and Notch3 mutant primers and HEX labeled *Notch3* and FAM labeled *Notch3*$^{6691\text{-}TAATGA}$ probes (Table 1B) (BioRad) at 95°C for 10 secs then 60°C for 30 secs and repeated for 45 cycles [53]. *Notch3* or *Notch3*$^{6691\text{-}TAATGA}$ mutant transcript copy number was estimated by comparison to a serial dilution of a 100 to 200 base pair (bp) synthetic DNA fragment (IDT) with or without the 6691TAATGA mutation in the *Notch3* locus cloned into pcDNA3.1(−) and copy number was corrected for *Rpl38* expression [52].

2.8 Statistics

Data are expressed as individual sample values, and as means ± SD. Data represent biological replicates except for osteoblast-enriched and stromal cell cultures, which represent technical replicates. qRT-PCR values were derived from two technical replicates of technical or biological replicates as indicated in the text and legends. Statistical differences were determined by unpaired *t* test for pairwise comparisons or two-way analysis of variance for multiple comparisons with Holm Šidák post-hoc analysis using GraphPad Prism version 9.3.1 for Mac OS, GraphPad Software (San Diego, CA).

3. RESULTS

3.1 Effect of Notch3 ASOs on Notch3 Expression in Cells of the Osteoblast Lineage

Twenty-four ASOs to target the *Notch3*$^{6691\text{-}TTATGA}$ mutation were synthesized and tested initially for toxicity *in vivo* following their administration to *BALB/c* mice at 50 mg/Kg/week for 4.5 weeks. Most of the ASOs tested were well tolerated in mice, with only a few showing mild elevation in liver transaminase levels (Figure 2). We selected 12 safe ASOs and examined them further for activity and specificity *in vitro* (Table 2). The effect of Notch3 mutant ASOs was tested in cells of the osteoblast lineage from *Notch3*^{em1Ecan} mice since previous work demonstrated that *Notch3* is preferentially expressed in cells of this lineage including osteocytes [12, 17, 54]. Five of the 12 ASOs tested decreased *Notch3*$^{6691\text{-}TAATGA}$ mRNA by ~60% to 100% 72 h after the addition of the ASO at 20 μM to the culture medium of osteoblast- enriched cells from *Notch3*^{em1Ecan} mice (Table 2). The effect of three ASOs (ASO14; ASO17; ASO18) was specific to the mutant *Notch3* mRNA since these ASOs did not downregulate *Notch3* wild type mRNA (Figure 3). These three ASOs were studied further, and ASO18 was tested at multiple doses to confirm the downregulation of *Notch3*$^{6691\text{-}TAATGA}$ mutant transcripts. Notch3 mutant ASO18 at 1 to 20 μM for 72 h downregulated *Notch3*$^{6691\text{-}TAATGA}$ mRNA 80% to 100% in *Notch3*^{em1Ecan} osteoblasts and did not alter the expression of *Notch1*, *Notch2*, wild type *Notch3* or *Notch 4* mRNA (Figure 4, Panels A and B). In addition, this Notch3 mutant ASO downregulated *Notch3*^{6691TAATGA} transcripts by 65% without affecting *Notch3* mRNA in cultures of bone marrow stromal cells (Figure 4, Panel C) confirming the effect observed in calvarial

osteoblasts. As expected, the *Notch3*^{6691TAATGA} transcript was not detected in control wild type cells.

3.2 Effect of Notch3 Mutant ASO on General Characteristics and Femoral Microarchitecture of Notch3^{em1Ecan} Mice

Heterozygous *Notch3*^{em1Ecan} mutant male mice were compared to wild type sex-matched littermate controls in a C57BL/6 genetic background. Male mice were studied since they have an osteopenic phenotype that is sustained for up to 3 to 4 months of age whereas female *Notch3*^{em1Ecan} mutants tend to have a more transient osteopenia [17]. Homozygous *Notch3*^{em1Ecan} mice were not studied since the homozygous mutation is developmentally lethal [17]. Three of the Notch3 mutant ASOs that suppressed *Notch3*$^{6691\text{-}TAATGA}$ transcripts *in vitro* specifically (Figure 3) were tested for their effects *in vivo* and were tolerated well without overt signs of toxicity. Two of 3 Notch3 mutant ASOs had no effect or inconsistent effects on the cancellous or cortical bone osteopenia of *Notch3*^{em1Ecan} mice and were not studied further (data not shown).

Mouse Notch3 mutant ASO18 or control ASO were administered once a week at 50 mg/Kg for 4 weeks. Notch3 mutant ASO18 was administered to 26 *Notch3*^{em1Ecan} mice and to 32 wild type littermates, and Notch3 control ASO was administered to 23 *Notch3*^{em1Ecan} mice and 34 control littermates. The weight of *Notch3*^{em1Ecan} heterozygous male mice was not different from those of control wild type mice and the femoral length was slightly decreased in *Notch3*^{em1Ecan} mice. These parameters were not altered by the administration of the Notch3 mutant ASO compared to control ASO. The administration of the Notch3 mutant ASO for a 4-week period decreased *Notch3*$^{6691\text{-}TAATGA}$ mRNA expression by ~50% in tibiae from *Notch3*^{em1Ecan} mutant mice without affecting *Notch3* mRNA (Figure 5). In accordance with previous observations, μCT of the femoral mid-diaphysis revealed that 2 month old *Notch3*^{em1Ecan} male mice had decreased cortical bone volume/total volume (BV/TV) associated with a 26% increase in porosity, a 18% decrease in cortical thickness and a 9% decrease in polar moment of inertia (Figure 6) [17]. The administration of the Notch3 mutant ASO increased cortical BV/TV and resulted in a 8% increase in cortical thickness and a 6% decrease in cortical porosity in *Notch3*^{em1Ecan} mice. In addition, when compared to control ASO, the Notch3 mutant ASO increased polar moment of inertia in *Notch3*^{em1Ecan} mice by 16% (p 0.07 by ANOVA; $p < 0.05$ by unpaired t-test), indicating an amelioration of skeletal fragility. No effect was noted in wild type mice by the administration of Notch3 ASO since the ASO was designed to target the *Notch3* mutation. Cancellous bone microarchitecture demonstrated that *Notch3*^{em1Ecan} mice had a 37% decrease in cancellous BV/TV and in trabecular number when compared to wild type littermates (Figure 6). Administration of Notch3 mutant ASO did not increase femoral BV/TV significantly in *Notch3*^{em1Ecan} (16%) mice and had no effect on control littermates (Figure 7). Therefore, the effect of the Notch3 mutant ASO was restricted to the cortical bone osteopenia of *Notch3*^{em1Ecan} mice.

4. DISCUSSION

The current work was undertaken to determine whether ASOs could be developed to target and downregulate a *Notch3* mutation in a mouse model (*Notch3*^{em1Ecan}) replicating the genetic variant found in LMS. Because *Notch3*^{em1Ecan} mice present with osteopenia, as a therapeutic end point we tested whether an improvement in genetic outcome would translate in amelioration of this aspect of the *Notch3*^{em1Ecan} phenotype. About 50% of the Notch3 mutant specific ASOs designed were found not to be toxic *in vivo* and were studied further for their activity in skeletal cells. Three of the 12 ASOs considered safe downregulated the *Notch3*$^{6691\text{-}TAATGA}$ mutation specifically without an effect on wild type *Notch3* transcripts in osteoblast cultures. One of the ASOs was pursued in detail and found to inhibit *Notch3* mutant transcripts *in vivo* and ameliorate phenotypic manifestations of *Notch3*^{em1Ecan} mice.

Although a variety of approaches to downregulate Notch signaling have been reported, they often are not specific to Notch activity or to a specific Notch receptor. Anti-Notch antibodies targeting the NRR are an exception and we have demonstrated that anti-NOTCH2 NRR and anti-NOTCH3 NRR antibodies are effective in reversing the skeletal phenotype of *Notch2*$^{tm1.1Ecan}$ and of *Notch3*^{em1Ecan} mice, models of Hajdu Cheney Syndrome and LMS, respectively [25, 26]. Although anti-Notch NRR antibodies are effective in their ability to downregulate a specific Notch receptor, they do not discriminate between the wild type and mutant forms of the Notch receptor. They induce substantial downregulation of Notch signaling with a potential of gastrointestinal toxicity. Because of these reasons, we search for other alternatives to reverse/ameliorate skeletal phenotypes associated with *Notch2* or *Notch3* mutations.

We demonstrated that Notch2 ASOs downregulate *Notch2* expression *in vitro* and *in vivo* and ameliorate the osteopenia of mice harboring a *Notch2* mutation replicating the one found in HCS [36]. Similarly, we found that Notch3 ASOs targeting *Notch3* downregulate *Notch3* wild type and mutant transcripts and ameliorate the cortical osteopenia of *Notch3*^{em1Ecan} mice [39].

The current approach was designed to target the *Notch3*$^{6691\text{-}TAATGA}$ mutation specifically in a heterozygous mouse model that replicates the genetic variant of LMS with the intent to preserve the activity of the wild type allele and create a state of functional normality. This approach would seem ideal for the targeting of mutations found in monogenic disorders with dominant inheritance, such as LMS. The downregulation of the *Notch3* mutant transcript by the Notch3 ASO was effective in *in vitro* models and *in vivo* it ameliorated the cortical osteopenia of *Notch3*^{em1Ecan} mice. However, Notch3 mutant ASOs did not modify significantly the cancellous bone osteopenia of *Notch3*^{em1Ecan} mice. The present study limited the administration of the Notch3 mutant specific ASO to 50 mg/Kg for a 4-week period, and it is possible that a longer period of administration could have a greater beneficial effect on the bone microarchitecture of *Notch3*^{em1Ecan} mice. The effect of Notch3 mutant ASOs *in vivo* was similar to the one that we reported recently on the effect of Notch3 ASOs. It is possible that Notch3 ASOs are more effective in the cortical compartment which is rich in osteocytes because *Notch3* is preferentially expressed in this cellular environment [12, 16, 54, 55]. It is also possible that ASOs are transported more efficiently to cortical

than to trabecular bone since the blood vessel network differs between these two skeletal compartments. A central nutrient artery and periosteal arteries irrigate cortical long bones, whereas epiphyseal arteries irrigate metaphyseal, cancellous-rich bone [56, 57]. However, perfusion efficiency studies do not reveal apparent differences between epiphyseal and diaphyseal bone vascularization [58].

Although the subcutaneous administration of Notch3 ASOs is practical from a possible therapeutic point of view, the present and prior studies suggest that ASOs are partially effective in the downregulation of the *Notch3* mutant transcripts in skeletal tissue and the reversal of skeletal phenotypes. Greater efficacy might be attained by enhancing the transport of the ASO to the target cell [59]. This has been achieved for skeletal muscle by conjugating ASOs to antigen binding fragments to the transferrin receptor 1 [60]. Although our study demonstrates amelioration of the cortical osteopenia in a mouse model that harbors a genetic variant found in LMS, there was not complete reversal of the phenotype. Future work developing strategies to target ASOs to specific skeletal cells may serve to improve their efficacy and potential therapeutic outcomes.

The present findings confirm that a mouse model replicating a mutation found in LMS displays femoral cancellous and cortical bone osteopenia [17]. There are some limitations of this study. The phenotype of the *Notch3*^{em1Ecan} mutant mouse recapitulates aspects of LMS including osteopenia, but not the neurological manifestations of the disease [16, 17]. Because only male mice were reported in the present study, it is important not to extrapolate the results observed to female mice. Phenotypic alterations of experimental and control mice were assessed by μCT, and analyses required the *ex vivo* exam of bone following the sacrifice of mice. Therefore, the same animal could not be analyzed before and after the administration of Notch3 ASOs. Cells were obtained from mice of both sexes for *in vitro* experiments since sex cell specific culture is at times impractical. The effects of Notch3 ASOs were assessed in cells of the osteoblast lineage and not in the myeloid/osteoclast lineage because *Notch3* is not expressed in this lineage and NOTCH3 does not have direct effects on osteoclastogenesis [3, 16, 17].

5. CONCLUSIONS

In conclusion, a Notch3 mutant ASO downregulated *Notch3* mutant expression specifically and ameliorated the cortical osteopenia of a mouse model that replicates the genetic variant found in LMS.

ACKNOWLEDGMENTS

The authors thank Mary Yurczak for secretarial support, and Emily Denker for technical assistance and creating figures for the manuscript.

This work was supported by the National Institute of Arthritis and Musculoskeletal and Skin Diseases (NIAMS) [grant numbers AR076747 and AR072987]. The content is solely the responsibility of the authors and does not necessarily represent the official views of the National Institutes of Health.

ABBREVIATIONS

α-MEM	α-minimum essential medium

ASO	antisense oligonucleotide
bp	base pair
BV/TV	bone volume/total volume
CADASIL	cerebral autosomal dominant arteriopathy with subcortical infarcts and leukoencephalopathy
cEt	constrained ethyl
DMEM	Dulbecco's modified Eagle's medium
FBS	fetal bovine serum
HES	Hairy Enhancer of Split
HEY	HES-related with YRPM
LMS	Lehman Syndrome or Lateral Meningocele Syndrome
μCT	microcomputed tomography
NRR	negative regulatory region
NICD	NOTCH intracellular domain
PS	phosphorothiate
pMOI	polar moment of inertia
PEST	proline (P), glutamic acid (E), serine (S) and threonine (T)
qRT-PCR	quantitative reverse transcript-polymerase chain reaction

REFERENCES

[1]. Siebel C, Lendahl U, Notch Signaling in Development, Tissue Homeostasis, and Disease, Physiol. Rev 97(4) (2017) 1235–1294. 10.1152/physrev.00005.2017 [PubMed: 28794168]

[2]. Zanotti S, Canalis E, Notch Signaling and the Skeleton, Endocr. Rev 37(3) (2016) 223–253. 10.1210/er.2016-1002 [PubMed: 27074349]

[3]. Canalis E, Notch in skeletal physiology and disease, Osteoporos.Int 29(12) (2018) 2611–2621. 10.1007/s00198-018-4694-3 [PubMed: 30194467]

[4]. Kovall RA, More complicated than it looks: assembly of Notch pathway transcription complexes, Oncogene 27(38) (2008) 5099–5109. [PubMed: 18758478]

[5]. Nam Y, Sliz P, Song L, Aster JC, Blacklow SC, Structural basis for cooperativity in recruitment of MAML coactivators to Notch transcription complexes, Cell 124(5) (2006) 973–983. [PubMed: 16530044]

[6]. Wilson JJ, Kovall RA, Crystal structure of the CSL-Notch-Mastermind ternary complex bound to DNA, Cell 124(5) (2006) 985–996. [PubMed: 16530045]

[7]. Iso T, Kedes L, Hamamori Y, HES and HERP families: multiple effectors of the Notch signaling pathway, J. Cell. Physiol 194(3) (2003) 237–255. 10.1002/jcp.10208 [PubMed: 12548545]

[8]. Liu H, Zhang W, Kennard S, Caldwell RB, Lilly B, Notch3 is critical for proper angiogenesis and mural cell investment, Circ Res 107(7) (2010) 860–870. 10.1161/CIRCRESAHA.110.218271 [PubMed: 20689064]

[9]. Mizuno T, Mizuta I, Watanabe-Hosomi A, Mukai M, Koizumi T, Clinical and Genetic Aspects of CADASIL, Front Aging Neurosci 12 (2020) 91. 10.3389/fnagi.2020.00091 [PubMed: 32457593]

[10]. Prakash N, Hansson E, Betsholtz C, Mitsiadis T, Lendahl U, Mouse Notch 3 expression in the pre- and postnatal brain: relationship to the stroke and dementia syndrome CADASIL, Exp. Cell Res 278(1) (2002) 31–44. 10.1006/excr.2002.5544 [PubMed: 12126955]

[11]. Henshall TL, Keller A, He L, Johansson BR, Wallgard E, Raschperger E, Mae MA, Jin S, Betsholtz C, Lendahl U, Notch3 is necessary for blood vessel integrity in the central nervous system, Arterioscler Thromb Vasc Biol 35(2) (2015) 409–420. 10.1161/ATVBAHA.114.304849 [PubMed: 25477343]

[12]. Canalis E, Zanotti S, Schilling L, Eller T, Yu J, Activation of Notch3 in osteoblasts/osteocytes causes compartment-specific changes in bone remodeling, J. Biol. Chem 296 (2021) 100583. 10.1016/j.jbc.2021.100583 [PubMed: 33774049]

[13]. Gripp KW, Scott CI Jr., Hughes HE, Wallerstein R, Nicholson L, States L, Bason LD, Kaplan P, Zderic SA, Duhaime AC, Miller F, Magnusson MR, Zackai EH, Lateral meningocele syndrome: three new patients and review of the literature, Am. J. Med. Genet 70(3) (1997) 229–239. [PubMed: 9188658]

[14]. Gripp KW, Robbins KM, Sobreira NL, Witmer PD, Bird LM, Avela K, Makitie O, Alves D, Hogue JS, Zackai EH, Doheny KF, Stabley DL, Sol-Church K, Truncating mutations in the last exon of NOTCH3 cause lateral meningocele syndrome, Am. J. Med. Genet. A 167A(2) (2015) 271–281. 10.1002/ajmg.a.36863 [PubMed: 25394726]

[15]. Lehman RA, Stears JC, Wesenberg RL, Nusbaum ED, Familial osteosclerosis with abnormalities of the nervous system and meninges, J. Pediatr 90(1) (1977) 49–54. [PubMed: 830893]

[16]. Canalis E, The Skeleton of Lateral Meningocele Syndrome, Front Genet 11 (2020) 620334. 10.3389/fgene.2020.620334 [PubMed: 33519922]

[17]. Canalis E, Yu J, Schilling L, Yee SP, Zanotti S, The lateral meningocele syndrome mutation causes marked osteopenia in mice, J. Biol. Chem 293(36) (2018) 14165–14177. 10.1074/jbc.RA118.004242 [PubMed: 30042232]

[18]. Ryeom SW, The cautionary tale of side effects of chronic Notch1 inhibition, J. Clin. Invest 121(2) (2011) 508–509. [PubMed: 21266769]

[19]. De Strooper B, Annaert W, Cupers P, Saftig P, Craessaerts K, Mumm JS, Schroeter EH, Schrijvers V, Wolfe MS, Ray WJ, Goate A, Kopan R, A presenilin-1-dependent gamma-secretase-like protease mediates release of Notch intracellular domain, Nature 398(6727) (1999) 518–522. 10.1038/19083 [PubMed: 10206645]

[20]. Duggan SP, McCarthy JV, Beyond gamma-secretase activity: The multifunctional nature of presenilins in cell signalling pathways, Cell. Signal 28(1) (2016) 1–11. 10.1016/j.cellsig.2015.10.006

[21]. Ilagan MX, Kopan R, Selective blockade of transport via SERCA inhibition: the answer for oncogenic forms of Notch?, Cancer Cell 23(3) (2013) 267–269. 10.1016/j.ccr.2013.02.020 [PubMed: 23518343]

[22]. Moellering RE, Cornejo M, Davis TN, Del BC, Aster JC, Blacklow SC, Kung AL, Gilliland DG, Verdine GL, Bradner JE, Direct inhibition of the NOTCH transcription factor complex, Nature 462(7270) (2009) 182–188. [PubMed: 19907488]

[23]. Lehal R, Zaric J, Vigolo M, Urech C, Frismantas V, Zangger N, Cao L, Berger A, Chicote I, Loubery S, Choi SH, Koch U, Blacklow SC, Palmer HG, Bornhauser B, Gonzalez-Gaitan M, Arsenijevic Y, Zoete V, Aster JC, Bourquin JP, Radtke F, Pharmacological disruption of the Notch transcription factor complex, Proc. Natl. Acad. Sci. U. S. A 117(28) (2020) 16292–16301. 10.1073/pnas.1922606117 [PubMed: 32601208]

[24]. Wu Y, Cain-Hom C, Choy L, Hagenbeek TJ, de Leon GP, Chen Y, Finkle D, Venook R, Wu X, Ridgway J, Schahin-Reed D, Dow GJ, Shelton A, Stawicki S, Watts RJ, Zhang J, Choy R, Howard P, Kadyk L, Yan M, Zha J, Callahan CA, Hymowitz SG, Siebel CW, Therapeutic antibody targeting of individual Notch receptors, Nature 464(7291) (2010) 1052–1057. 10.1038/nature08878 [PubMed: 20393564]

[25]. Canalis E, Sanjay A, Yu J, Zanotti S, An Antibody to Notch2 Reverses the Osteopenic Phenotype of Hajdu-Cheney Mutant Male Mice, Endocrinology 158(4) (2017) 730–742. 10.1210/en.2016-1787 [PubMed: 28323963]

[26]. Yu J, Siebel CW, Schilling L, Canalis E, An antibody to Notch3 reverses the skeletal phenotype of lateral meningocele syndrome in male mice, J. Cell. Physiol 235(1) (2020) 210–220. 10.1002/jcp.28960 [PubMed: 31188489]

[27]. Murray SF, Jazayeri A, Matthes MT, Yasumura D, Yang H, Peralta R, Watt A, Freier S, Hung G, Adamson PS, Guo S, Monia BP, LaVail MM, McCaleb ML, Allele-Specific Inhibition of Rhodopsin With an Antisense Oligonucleotide Slows Photoreceptor Cell Degeneration, Invest Ophthalmol Vis Sci 56(11) (2015) 6362–6375. 10.1167/iovs.15-16400 [PubMed: 26436889]

[28]. Shy ME, Antisense oligonucleotides offer hope to patients with Charcot-Marie-Tooth disease type 1A, J. Clin. Invest 128(1) (2018) 110–112. 10.1172/JCI98617 [PubMed: 29199996]

[29]. Carroll JB, Warby SC, Southwell AL, Doty CN, Greenlee S, Skotte N, Hung G, Bennett CF, Freier SM, Hayden MR, Potent and selective antisense oligonucleotides targeting single-nucleotide polymorphisms in the Huntington disease gene / allele-specific silencing of mutant huntingtin, Mol. Ther 19(12) (2011) 2178–2185. 10.1038/mt.2011.201 [PubMed: 21971427]

[30]. Limmroth V, Barkhof F, Desem N, Diamond MP, Tachas G, Group ATLS, CD49d antisense drug ATL1102 reduces disease activity in patients with relapsing-remitting MS, Neurology 83(20) (2014) 1780–1788. 10.1212/WNL.0000000000000926 [PubMed: 25239835]

[31]. McCampbell, Cole T, Wegener AJ, Tomassy GS, Setnicka A, Farley BJ, Schoch KM, Hoye ML, Shabsovich M, Sun L, Luo Y, Zhang M, Comfort N, Wang B, Amacker J, Thankamony S, Salzman DW, Cudkowicz M, Graham DL, Bennett CF, Kordasiewicz HB, Swayze EE, Miller TM, Antisense oligonucleotides extend survival and reverse decrement in muscle response in ALS models, J. Clin. Invest 128(8) (2018) 3558–3567. 10.1172/JCI99081 [PubMed: 30010620]

[32]. Zhao HT, Damle S, Ikeda-Lee K, Kuntz S, Li J, Mohan A, Kim A, Hung G, Scheideler MA, Scherer SS, Svaren J, Swayze EE, Kordasiewicz HB, PMP22 antisense oligonucleotides reverse Charcot-Marie-Tooth disease type 1A features in rodent models, J. Clin. Invest 128(1) (2018) 359–368. 10.1172/JCI96499 [PubMed: 29202483]

[33]. Zhu C, Kim K, Wang X, Bartolome A, Salomao M, Dongiovanni P, Meroni M, Graham MJ, Yates KP, Diehl AM, Schwabe RF, Tabas I, Valenti L, Lavine JE, Pajvani UB, Hepatocyte Notch activation induces liver fibrosis in nonalcoholic steatohepatitis, Sci Transl Med 10(468) (2018) 10.1126/scitranslmed.aat0344

[34]. Li M, Jancovski N, Jafar-Nejad P, Burbano LE, Rollo B, Richards K, Drew L, Sedo A, Heighway J, Pachernegg S, Soriano A, Jia L, Blackburn T, Roberts B, Nemiroff A, Dalby K, Maljevic S, Reid CA, Rigo F, Petrou S, Antisense oligonucleotide therapy reduces seizures and extends life span in an SCN2A gain-of-function epilepsy model, J. Clin. Invest 131(23) (2021) 10.1172/JCI152079

[35]. Nguyen Q, Yokota T, Antisense oligonucleotides for the treatment of cardiomyopathy in Duchenne muscular dystrophy, Am J Transl Res 11(3) (2019) 1202–1218. [PubMed: 30972156]

[36]. Canalis E, Grossman TR, Carrer M, Schilling L, Yu J, Antisense oligonucleotides targeting Notch2 ameliorate the osteopenic phenotype in a mouse model of Hajdu-Cheney syndrome, J. Biol. Chem 295(12) (2020) 3952–3964. 10.1074/jbc.RA119.011440 [PubMed: 31992595]

[37]. Bennett CF, Baker BF, Pham N, Swayze E, Geary RS, Pharmacology of Antisense Drugs, Annu. Rev. Pharmacol. Toxicol 57 (2017) 81–105. 10.1146/annurev-pharmtox-010716-104846 [PubMed: 27732800]

[38]. Cerritelli SM, Crouch RJ, Ribonuclease H: the enzymes in eukaryotes, FEBS J. 276(6) (2009) 1494–1505. 10.1111/j.1742-4658.2009.06908.x [PubMed: 19228196]

[39]. Canalis E, Carrer M, Eller T, Schilling L, Yu J, Use of antisense oligonucleotides to target Notch3 in skeletal cells, PLoS One 17(5) (2022) e0268225. 10.1371/journal.pone.0268225 [PubMed: 35536858]

[40]. Vasquez G, Freestone GC, Wan WB, Low A, De Hoyos CL, Yu J, Prakash TP, Ostergaard ME, Liang XH, Crooke ST, Swayze EE, Migawa MT, Seth PP, Site-specific incorporation of 5'-methyl DNA enhances the therapeutic profile of gapmer ASOs, Nucleic Acids Res. 49(4) (2021) 1828–1839. 10.1093/nar/gkab047 [PubMed: 33544849]

[41]. Yesil P, Michel M, Chwalek K, Pedack S, Jany C, Ludwig B, Bornstein SR, Lammert E, A new collagenase blend increases the number of islets isolated from mouse pancreas, Islets 1(3) (2009) 185–190. 10.4161/isl.1.3.9556 [PubMed: 21099271]

[42]. McCarthy TL, Centrella M, Canalis E, Further biochemical and molecular characterization of primary rat parietal bone cell cultures, J. Bone Miner. Res 3(4) (1988) 401–408. [PubMed: 3265577]

[43]. Zanotti S, Kalajzic I, Aguila HL, Canalis E, Sex and genetic factors determine osteoblastic differentiation potential of murine bone marrow stromal cells, PLoS One 9(1) (2014) e86757. 10.1371/journal.pone.0086757 [doi];PONE-D-13–31354 [pii] [PubMed: 24489784]

[44]. Bouxsein ML, Boyd SK, Christiansen BA, Guldberg RE, Jepsen KJ, Muller R, Guidelines for assessment of bone microstructure in rodents using micro-computed tomography, J. Bone Miner. Res 25(7) (2010) 1468–1486. [PubMed: 20533309]

[45]. Glatt V, Canalis E, Stadmeyer L, Bouxsein ML, Age-Related Changes in Trabecular Architecture Differ in Female and Male C57BL/6J Mice, J. Bone Miner. Res 22(8) (2007) 1197–1207. [PubMed: 17488199]

[46]. Canalis E, Schilling L, Yee SP, Lee SK, Zanotti S, Hajdu Cheney Mouse Mutants Exhibit Osteopenia, Increased Osteoclastogenesis and Bone Resorption, J. Biol. Chem 291 (2016) 1538–1551. 10.1074/jbc.M115.685453 [PubMed: 26627824]

[47]. Zanotti S, Yu J, Sanjay A, Schilling L, Schoenherr C, Economides AN, Canalis E, Sustained Notch2 signaling in osteoblasts, but not in osteoclasts, is linked to osteopenia in a mouse model of Hajdu-Cheney syndrome, J. Biol. Chem 292(29) (2017) 12232–12244. 10.1074/jbc.M117.786129 [PubMed: 28592489]

[48]. Nazarenko, Lowe B, Darfler M, Ikonomi P, Schuster D, Rashtchian A, Multiplex quantitative PCR using self-quenched primers labeled with a single fluorophore, Nucleic Acids Res. 30(9) (2002) e37. [PubMed: 11972352]

[49]. Nazarenko, Pires R, Lowe B, Obaidy M, Rashtchian A, Effect of primary and secondary structure of oligodeoxyribonucleotides on the fluorescent properties of conjugated dyes, Nucleic Acids Res. 30(9) (2002) 2089–2195. [PubMed: 11972350]

[50]. Nye JS, Kopan R, Axel R, An activated Notch suppresses neurogenesis and myogenesis but not gliogenesis in mammalian cells, Development 120(9) (1994) 2421–2430. [PubMed: 7956822]

[51]. Shirayoshi Y, Yuasa Y, Suzuki T, Sugaya K, Kawase E, Ikemura T, Nakatsuji N, Proto-oncogene of int-3, a mouse Notch homologue, is expressed in endothelial cells during early embryogenesis, Genes Cells 2(3) (1997) 213–224. [PubMed: 9189758]

[52]. Gibson DG, Young L, Chuang RY, Venter JC, Hutchison CA 3rd, Smith HO, Enzymatic assembly of DNA molecules up to several hundred kilobases, Nat. Methods 6(5) (2009) 343–345. 10.1038/nmeth.1318 [PubMed: 19363495]

[53]. Kutyavin IV, Afonina IA, Mills A, Gorn VV, Lukhtanov EA, Belousov ES, Singer MJ, Walburger DK, Lokhov SG, Gall AA, Dempcy R, Reed MW, Meyer RB, Hedgpeth J, 3'-minor groove binder-DNA probes increase sequence specificity at PCR extension temperatures, Nucleic Acids Res. 28(2) (2000) 655–661. [PubMed: 10606668]

[54]. Zanotti S, Canalis E, Parathyroid hormone inhibits Notch signaling in osteoblasts and osteocytes, Bone 103 (2017) 159–167. 10.1016/j.bone.2017.06.027 [PubMed: 28676438]

[55]. Delgado-Calle J, Anderson J, Cregor MD, Hiasa M, Chirgwin JM, Carlesso N, Yoneda T, Mohammad KS, Plotkin LI, Roodman GD, Bellido T, Bidirectional Notch Signaling and Osteocyte-Derived Factors in the Bone Marrow Microenvironment Promote Tumor Cell Proliferation and Bone Destruction in Multiple Myeloma, Cancer Res. 76(5) (2016) 1089–1100. 10.1158/0008-5472.CAN-15-1703 [PubMed: 26833121]

[56]. Filipowska J, Tomaszewski KA, Niedzwiedzki L, Walocha JA, Niedzwiedzki T, The role of vasculature in bone development, regeneration and proper systemic functioning, Angiogenesis 20(3) (2017) 291–302. 10.1007/s10456-017-9541-1 [PubMed: 28194536]

[57]. Watson EC, Adams RH, Biology of Bone: The Vasculature of the Skeletal System, Cold Spring Harb Perspect Med 8(7) (2018) a031559. 10.1101/cshperspect.a031559

[58]. Lassailly F, Foster K, Lopez-Onieva L, Currie E, Bonnet D, Multimodal imaging reveals structural and functional heterogeneity in different bone marrow compartments: functional

implications on hematopoietic stem cells, Blood 122(10) (2013) 1730–1740. 10.1182/blood-2012-11-467498 [PubMed: 23814020]

[59]. Zhang G, Guo B, Wu H, Tang T, Zhang BT, Zheng L, He Y, Yang Z, Pan X, Chow H, To K, Li Y, Li D, Wang X, Wang Y, Lee K, Hou Z, Dong N, Li G, Leung K, Hung L, He F, Zhang L, Qin L, A delivery system targeting bone formation surfaces to facilitate RNAi-based anabolic therapy, Nature medicine 18(2) (2012) 307–314. 10.1038/nm.2617

[60]. Desjardins CA, Yao M, Hall J, O'Donnell E, Venkatesan R, Spring S, Wen A, Hsia N, Shen P, Russo R, Lan B, Picariello T, Tang K, Weeden T, Zanotti S, Subramanian R, Ibraghimov-Beskrovnaya O, Enhanced exon skipping and prolonged dystrophin restoration achieved by TfR1-targeted delivery of antisense oligonucleotide using FORCE conjugation in mdx mice, Nucleic Acids Res. 50(20) (2022) 11401–11414. 10.1093/nar/gkac641 [PubMed: 35944903]

Highlights

- Lateral Meningocele Syndrome (LMS) is associated with *NOTCH3* mutations
- A mouse model of LMS (*Notch3*^{em1Ecan}) harbors a *Notch3* mutation and exhibits cortical and trabecular osteopenia
- Antisense oligonucleotides targeting the *Notch3* mutation in the mouse environment ameliorate the cortical osteopenia of *Notch3*^{em1Ecan} mice

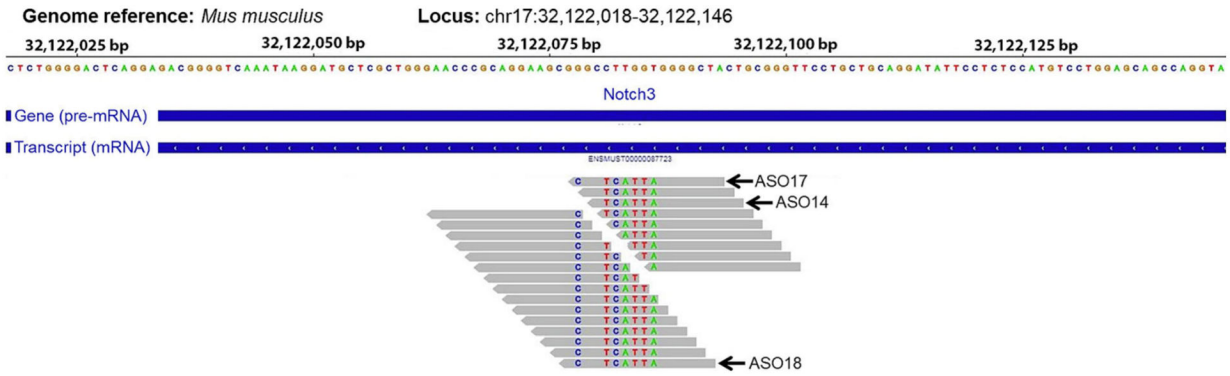

Figure 1.

Twenty-four ASOs were designed to target the mouse mutant *Notch3* pre-mRNA specifically and induce degradation of the LMS-causing transcript. Grey bars represent the site targeted by each ASO. The colored letters inside the grey bars represent the residues that are mutated in the LMS compared to the wild-type mouse Notch3 transcript. The wild-type mouse *Notch3* pre-mRNA sequence is reported at top of the figure. Arrows indicate the three ASOs studied in detail (ASO 14, 17 and 18).

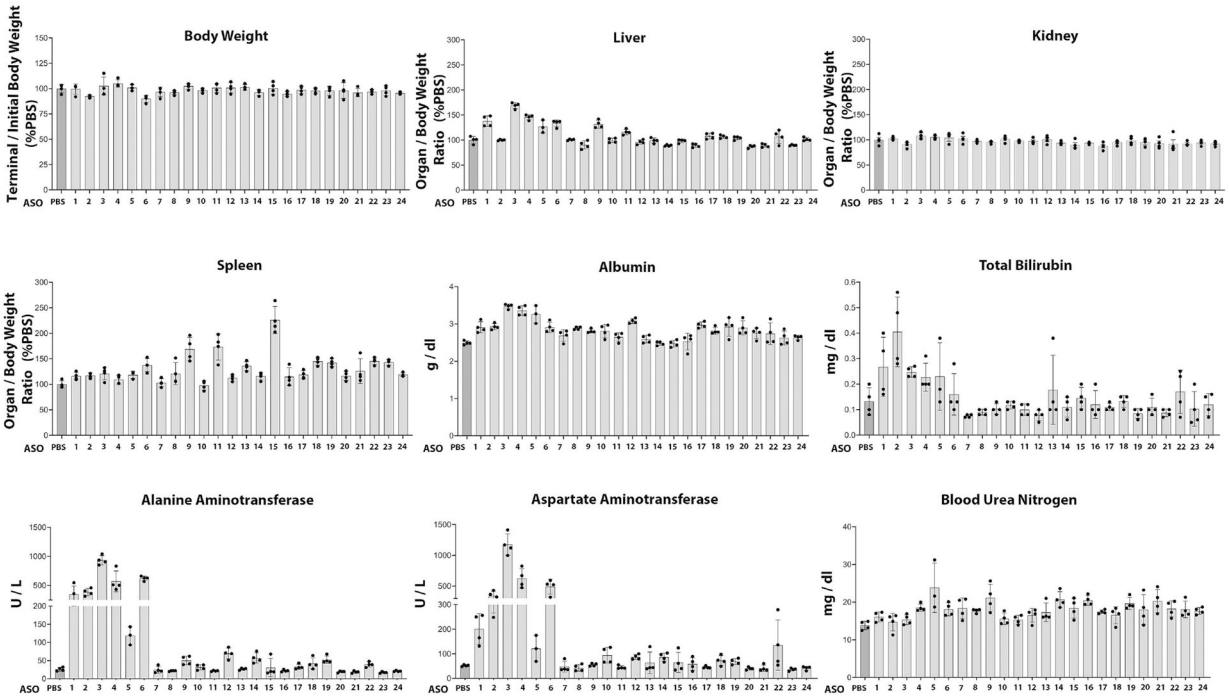

Figure 2.

The safety profile of 24 mutant Notch3 ASOs was evaluated in mice following subcutaneous administration once a week for 4.5 weeks at 50 mg/Kg. At the end of the study, body, liver, kidney, and spleen weights were assessed, and plasma levels of alanine aminotransferase, aspartate aminotransferase, total bilirubin, albumin, and blood urea nitrogen were measured. Individual values are shown, and bars and ranges represent means ± SD; n = 4 mice for each ASO tested. Twelve ASOs considered safe were selected for subsequent activity studies.

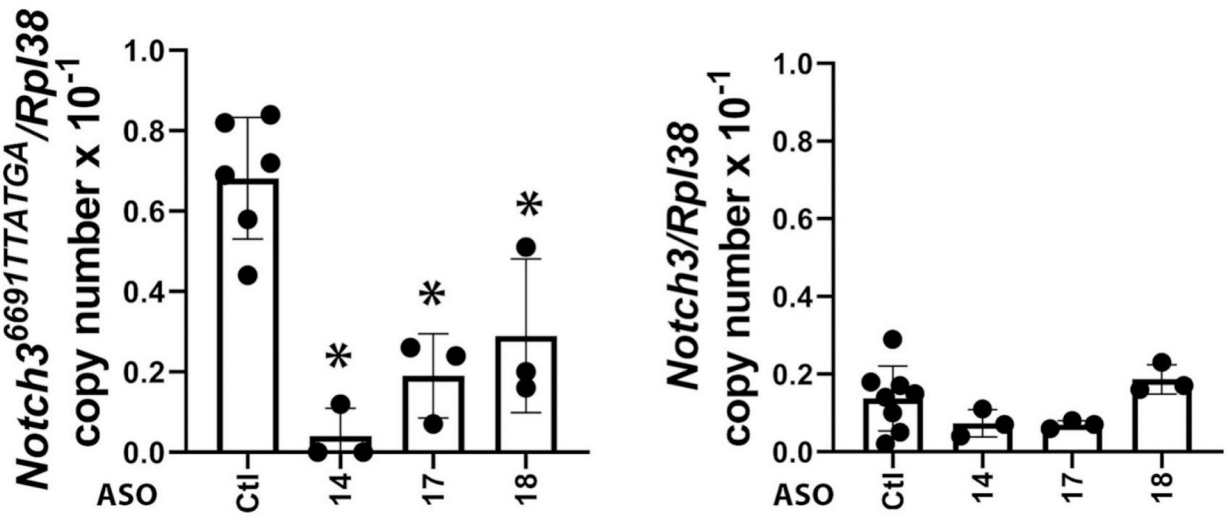

Figure 3.

Effect of control or Notch3 mutant ASOs (14, 17 and 18) on *Notch3* and *Notch3*$^{6691\text{-}TAATGA}$ mRNA expression in calvarial osteoblast-enriched cells from *Notch3*^{em1Ecan} mice. *Notch3* and *Notch3*$^{6691\text{-}TAATGA}$ mRNA levels were obtained 72 h after the addition of Notch3 mutant or control ASO at 20 μM to the culture medium. Transcript levels are expressed as copy number following correction for *Rpl38*. Individual values are shown, and bars and ranges represent means ± SD; n = 3 technical replicates. *Significantly different between Notch3 mutant ASO and control ASO by ANOVA with post-hoc analysis by Holm Šidák, $p < 0.05$.

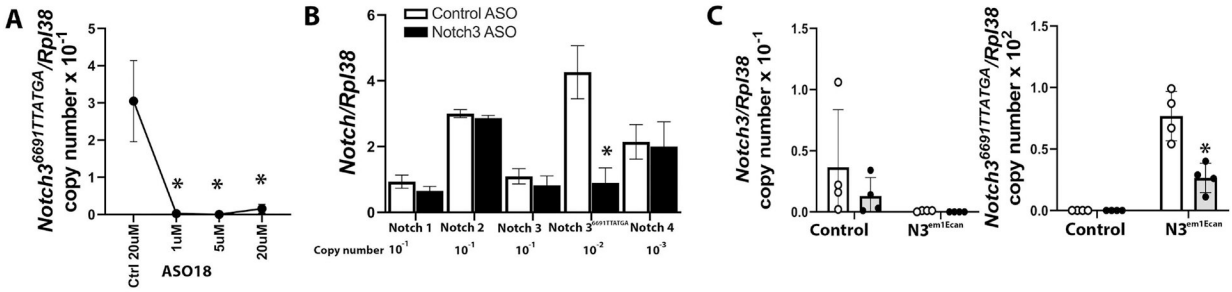

Figure 4.

Effect of control or Notch3 mutant ASO 18 on *Notch3*$^{6691\text{-}TAATGA}$ mRNA expression in calvarial osteoblast-enriched (A and B) and bone marrow stromal (C) cells from *Notch3*^{em1Ecan} mice. In Panel A, *Notch3*$^{6691\text{-}TAATGA}$ mRNA levels were obtained 72 h after the addition of Notch3 mutant or control ASO at the indicated doses. In Panel B, *Notch1*, *Notch2*, *Notch3*, *Notch3*$^{6691\text{-}TAATGA}$ and *Notch4* mRNA were detected 72 h after the addition of Notch3 mutant or control ASO at 20μM. In Panel C, *Notch3* and *Notch3*^{6691TAATGA} mRNA levels were obtained after the addition of Notch 3 mutant (closed circles grey bars,) or control ASO (open circles, white bars,) at 20μM for 72 h. Transcript levels are expressed as copy number following correction for *Rpl38*. In Panels A and B, values are means ± SD. In Panel C, individual values are shown, and bars and ranges represent mean ± SD; n = 3 or 4 technical replicates. *Significantly different between Notch3 mutant ASO and control ASO by ANOVA with post-hoc analysis by Holm Šidák (Panels A and C) or unpaired *t*-test (Panel B), $p < 0.05$.

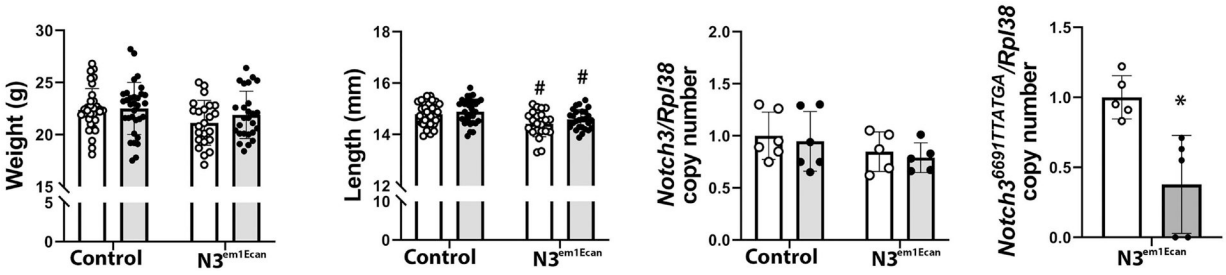

Figure 5.

Body weight, femoral length and Notch3 and *Notch3*$^{6691\text{-}TAATGA}$ transcripts in tibiae of 2-month-old male *Notch3*^{em1Ecan} mutant mice and littermate controls treated with Notch3 mutant ASO 18 (closed circles, grey bars) or control ASO (open circles, white bars) at 50 mg/Kg subcutaneously, once a week for 4 weeks. Individual values are shown, and bars and ranges represent means ± SD; n = 34 wild type mice treated with control ASO, n = 32 wild type mice treated with Notch3 ASO and n = 23 *Notch3*^{em1Ecan} mice treated with control ASO and n = 26 *Notch3*^{em1Ecan} mice treated with Notch3 mutant ASO, except for *Notch3*$^{6691\text{-}TAATGA}$ mRNA values n = 5 biological replicates. *Significantly different between Notch3 ASO and control, $p < 0.05$. #Significantly different between *Notch3*^{em1Ecan} mutant and control mice, $p < 0.05$, by ANOVA with post-hoc analysis by Holm Šidák or unpaired *t*-test for *Notch3*$^{6691\text{-}TAATGA}$ mRNA.

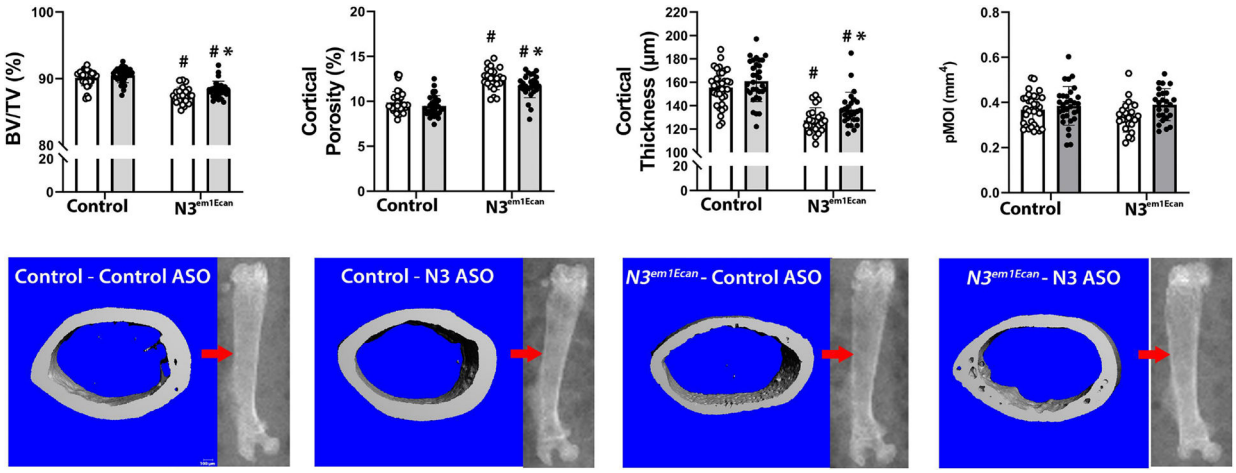

Figure 6.

Cortical bone microarchitecture assessed by μCT of the mid-diaphyseal femur from 2 month old *Notch3*^{em1Ecan} mutant male mice and sex-matched littermate controls treated with Notch3 mutant ASO 18 (closed circles, grey bars; n = 32 for wild type mice, n = 26 for *Notch3*^{em1Ecan}) or control ASO (open circles, white bars; n = 34 for wild type mice, n = 23 for *Notch3*^{em1Ecan}) both at 50 mg/Kg subcutaneously, once a week for 4 weeks prior to sacrifice. Parameters shown are cortical bone volume/total volume (BV/TV, %), cortical porosity (%), cortical thickness (mm) and polar moment of inertia (pMOI). Individual values are shown, and bars and ranges represent means ± SD of biological replicates. *Significantly different between Notch3 mutant and control ASO, $p < 0.05$. #Significantly different between *Notch3*^{em1Ecan} and control, $p < 0.05$, by ANOVA with post-hoc analysis by Holm Šidák. Representative images show cortical bone osteopenia in *Notch3*^{em1Ecan} mutant mice and its amelioration by Notch3 mutant ASOs. Scale bars in the right corner represent 100 μm. Arrow on scout μCT images point to the area analyzed.

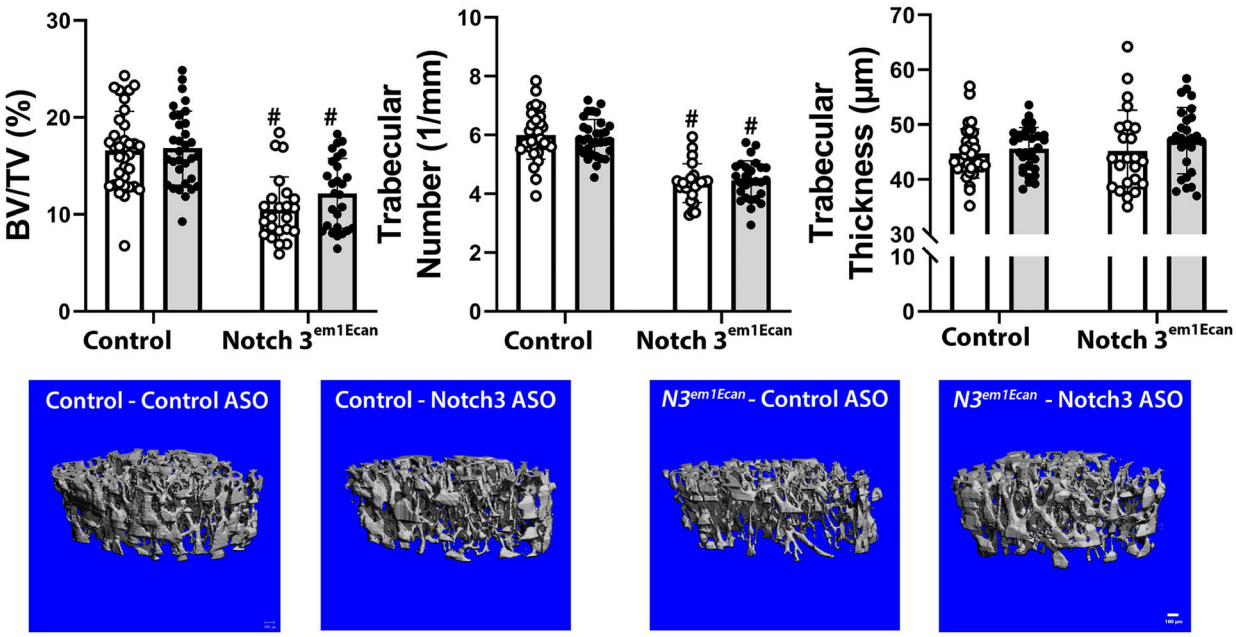

Figure 7.

Cancellous bone microarchitecture assessed by μCT of the distal femur from 2 month old *Notch3*^{em1Ecan} mutant male mice and sex-matched littermate controls treated with Notch3 mutant ASO 18 (closed circles, grey bars; n = 32 for wild type mice, n = 26 for *Notch3*^{em1Ecan}) or control ASO (open circles, white bars; n = 34 for wild type mice, n = 23 for *Notch3*^{em1Ecan}) both at 50 mg/Kg subcutaneously, once a week for 4 weeks prior to sacrifice. Parameters shown are trabecular bone volume/total volume (BV/TV, %); trabecular number (1/mm) and thickness (um). Individual values are shown, and bars and ranges represent means ± SD of biological replicates. #Significantly different between *Notch3*^{em1Ecan} and control, $p < 0.05$, by ANOVA with post-hoc analysis by Holm Šidák. Representative images show cancellous bone osteopenia in *Notch3*^{em1Ecan} mutant mice and no effect by Notch3 mutant ASO. Scale bars in the right corner represent 100 μm.

Table 1.

Primers used for qRT-PCR determinations. GenBank accession numbers identify transcript recognized by primer pairs.

A. Conventional qRT-PCR			
Gene	**Strand**	**Sequence**	**GenBank Accession Number**
Notch1	Forward Reverse	5'-GTCCCACCCATGACCACTACCCAGTTC-3' 5'-GGGTGTTGTCCACAGGGGA-3'	NM_008714
Notch2	Forward Reverse	5'-TGACGTTGATGAGTGTATCTCCAAGCC-3' 5'-GTAGCTGCCCTGAGTGTTGTGG-3'	NM_010928
Notch3[*]	Forward Reverse	5'-CCGATTCTCCTGTCGTTGTCTCC-3' 5'-TGAACACAGGGCCTGCTGAC-3'	NM_008716
Notch4	Forward Reverse	5'-CCAGCAGACAGACTACGGTGGAC-3' 5'-GCAGCCAGCATCAAAGGTGT-3'	NM_010929
Rpl38	Forward Reverse	5'-AGAACAAGGATAATGTGAAGTTCAAGGTTC-3' 5'-CTGCTTCAGCTTCTCTGCCTTT-3'	NM_001048057; NM_001048058; NM_023372
B. qRT-PCR using fluorescent tagged PCR products			
Gene	**Strand/Flurophore**	**Sequence**	**GenBank Accession Number**
Notch3	Forward Reverse HEX Fluorophore	5'-AGGACATGGAGAGGAATA-3' 5'-GGTCAAATAAGGATGCTC-3' 5'-ACCAAGGCCCGCTTCC-3'	Not Applicable
Notch3$^{6691\text{-}TAATGA}$	Forward Reverse FAM Fluorophore	5'-AGGACATGGAGAGGAATA-3' 5'-GGTCAAATAAGGATGCTC-3' 5'-AGTAGCCCCTAATGAGCGCG-3'	Not Applicable

[*] Used for Notch3 wild type mRNA determination in Figure 4, Panel B.

Table 2.

Screening of Notch3 mutant ASOs for activity *in vitro*.

ASO	Notch3 Downregulation	*Notch3*^{6691TAATGA} Downregulation
07	0%	0%
08	0%	0%
10	0%	0%
11	0%	0%
13	0%	0%
14	~15%	100%
16	~40%	100%
17	0%	70%
18	0%	60%
19	~40%	0%
20	~25%	0%
21	100%	100%

Twelve ASOs considered safe were tested at 20 μM for their effect on *Notch3* wild type or *Notch3*^{6691TAAGTA} mutant transcripts in osteoblast-enriched cells from *Notch3*^{em1Ecan} mice. Notch3 mutant ASOs that were not safe or borderline safe *in vivo* were not tested *in vitro*.